Intramolecular dynamics from a statistical analysis of vibrational levels: Application of two coupled Morse oscillator models to the HCN molecule

Fabio Pichierri,[1,*] Jair Botina,[1,2,†] and Naseem Rahman[1,‡]
[1]*Dipartimento di Scienze Chimiche dell' Università di Trieste, via L. Giorgieri 1, 34127 Trieste, Italy*
[2]*International Centre for Theoretical Physics, strada Costiera 11, 34136 Trieste, Italy*
(Received 30 January 1995)

Two local-mode model Hamiltonians containing stretch-stretch couplings have been utilized to obtain the vibrational energy levels of the HCN molecule for the purpose of studying them statistically. The effect of the kinetic coupling has been clearly obtained from the statistical analysis which includes nearest-neighbor level-spacing distributions (NNLSD) and the Δ_3 statistics of Dyson and Mehta. For NNLSD, a pronounced tendency towards the Wigner distribution has been found. The role of isotopic masses in the statistical properties of the vibrational spectra has also been elucidated. Comparison has been made between the results obtained from the two models. Correlation has been found between a transition to chaos (utilizing Poincaré sections and Lyapunov exponents) through classical mechanics and the above statistical behavior of the spectra.

PACS number(s): 31.15.Qq, 33.15.−c

I. INTRODUCTION

Polyatomic molecules have complex spectroscopic features arising from the interaction between electronic, vibrational, and rotational degrees of freedom. By employing pertinent factorizations of the total molecular wave function it is possible, however, to isolate part of the spectrum and concentrate on characteristics that arise specifically from one kind of motion. In the limits of the well-known Born-Oppenheimer approximation and due to the experimental limitations, most of the molecular spectroscopic activity has been focused on the lower-energy part of the potential energy surface (PES) where the description of the vibrational spectrum has been very effective in terms of normal modes (NM) [1,2]. There has been significant development in both experimental and theoretical research, in recent years, in order to take a close look at the higher-energy part of the PES, where the strong coupling between the vibrational degrees of freedom plays an important role. The most important consequence is that, due to the very high density of levels in this energy region of the spectra, the assignment of each energy level becomes rather complicated. The information that one obtains, while quantitative, in some sense does not give a broad general picture of the basic characteristics of the spectra [3,4]. Such a situation occurred in nuclear spectroscopy some time ago and the solution to the problem was given in terms of statistical analysis of the spectra [5]. It was found that certain trends in the statistical features of the spectra can be linked to the dynamics, thereby a global view of the spectra could be obtained. The same conclusions are now being drawn also for the vibrational spectra of polyatomic molecules in various recent studies [6–15]. First, experiments are being performed in the higher-energy part of the spectra, resulting in sufficient data for making statistical analysis. Second, theoretical vibrational spectra are being obtained by utilizing the local-mode (LM) description, which is more relevant and realistic at these energy domains [16–19]. With reasonable spectroscopic Hamiltonians, in the LM description, theoretical energy levels are obtained, they are made to satisfy accurately the energy eigenstates at the lower energies, and then their higher part is calculated. The statistical analysis of the entire spectrum is then done and it is either compared with exiting data or predictions are made for future experiments. Thus dynamics of molecular vibrations in an energy region which had not been looked at before begins to be elucidated at a level which has not been possible previously. In this context, we have shown recently how statistical properties of vibrational levels are affected by isotopic mass dependence of the constituent atoms [12–14] and by increasing molecular complexity of the polyatomic system under study [8,15]. The above considerations have to be, of course, applied to specific molecular systems which have been well studied so that the starting point for such research is reasonably secure. In this context, triatomic molecules represent molecular systems where the complex vibrational dynamics is determined by the presence of a minimum number of couplings between stretching and bending (local) modes. In this paper, we have chosen to subject the HCN molecule to such a study because of the experimental and theoretical information available for this molecule. Experimentally, it has been possible to study dispersed fluorescence [20], infrared overtone [21], and stimulated emission pumping spectra [22] of the HCN molecule and obtain a large amount of information from them. Furthermore, *ab initio* and empirical potential energy surfaces have been calculated [23–28] and both classical and quantum mechanical studies have been made regarding both spectra as well as the dynamics of the same molecule [29–33]. We have recently studied the problem of vibrational chaos classically [12], utilizing an accurate spectroscopic potential described below. A transition from regular dynamics to chaos has been seen between 2.8 and 2.9 eV calculating relevant Lyapunov exponents and Poincaré sections. Otherwise, little information is available regarding the vibrational energy levels in the higher-energy

*Electronic address: PICHIERR@UNIV. TRIESTE.IT
†Present address: Department of Chemistry, Princeton University, Princeton, NJ 08544.
‡Electronic address: RAHMAN@UNIV. TRIESTE.IT

region of the spectra. We believe that this theoretical description is accurate enough to explore its quantum features and make certain predictions of statistical nature for the higher-energy part of the vibrational spectra. This is done in this study. Furthermore, it appears that the experimental work will extend into this region in the near future, so that this study is rather relevant at this time.

II. COUPLED MORSE OSCILLATOR MODELS

A convenient description of the dynamics in the relatively high-energy regime is provided by a LM model, which explicitly considers the bonds and the relevant angles of the molecule. In the last years, a relatively large number of such local-mode vibrational Hamiltonians has become available from molecular spectroscopy and they have been utilized for statistical analysis of small polyatomic molecules [6–15]. For triatomic molecules, in the frozen-bending approximation, the Hamiltonian can in general be written as a sum of kinetic and potential energy terms,

$$H=T(p_1,p_2)+V(r_1,r_2)\ , \tag{1}$$

where

$$T(p_1,p_2)=\frac{p_1^2}{2\mu_1}+\frac{p_2^2}{2\mu_2}+\frac{\cos(\theta_{12})}{m_C}\,p_1p_2 \tag{2}$$

is the kinetic term with p_i $(i=1,2)$ the momenta of the two oscillators and μ_i $(i=1,2)$ the reduced masses, m_C the mass of the central carbon atom, and θ_{12} the angle between two bonds (for the HCN molecule θ_{12} is 180°). In this description only the kinetic part is analytic, while specific expressions for the potential function $V(r_1,r_2)$ are to be determined. For bending motion with a lower frequency than stretching, a good description of the vibrational dynamics may be given in terms of two coupled oscillators. The most realistic oscillator, which mimics this dynamics, is the Morse diatomic potential function [34]

$$V_M(r_i)=D_e(1-e^{-a_ir_i})^2 \quad (i=1,2)\ , \tag{3}$$

where D_e is the bond dissociation energy and r_i the bond displacement from the equilibrium position. Further improvements in this description have been made by molecular spectroscopists with empirically determined potential energy surfaces for some triatomic molecules, by fitting the spectra with an expansion in the Morse oscillator coordinate

$$z_i=(1-e^{-a_ir_i}) \quad (i=1,2)\ . \tag{4}$$

The number of terms utilized to express $V(r_1,r_2)$ depends on the quantity of the experimental levels to be fitted. One may rewrite the Hamiltonian as

$$H=H_1+H_2+H_{12}, \tag{5}$$

with H_i $(i=1,2)$ as unperturbed Hamiltonians and H_{12} being the interaction term. In our study we have chosen two different spectroscopic Hamiltonians, both based on the LM description, available for the HCN molecule. These are the so-called *simple Morse* (SM, model I) [25] and the *generalized Morse* (GM, model II) [26] model Hamiltonians.

Model I.

$$H_i=\frac{p_i^2}{2\mu_i}+V_{ii}z_i^2 \quad (i=1,2)\ , \tag{6}$$

$$H_{12}=\frac{\cos(\theta_{12})}{m_C}\,p_1p_2+V_{12}z_1z_2\ . \tag{7}$$

Model II.

$$H_i=\frac{p_i^2}{2\mu_i}+V_{ii}z_i^2+V_{iii}z_i^3+V_{iiii}z_i^4 \quad (i=1,2)\ , \tag{8}$$

$$H_{12}=\frac{\cos(\theta_{12})}{m_C}\,p_1p_2+V_{12}z_1z_2+V_{112}z_1^2z_2+V_{122}z_1z_2^2\ . \tag{9}$$

For both models $V_{ii}z_i^2$ $(i=1,2)$ correspond to the Morse potential $V_M(r_i)$ for the ith bond. These two Hamiltonians represent a good description for a large number of highly excited vibrational levels, in particular the SM model fits the first 20 levels and the GM model the first 40 levels from the ground vibrational state in a satisfactory manner. The parameters V_{ii} and V_{ij} are related to the internal harmonic stretching force constants [35] as follows:

$$f_{rr}=2V_{ii}a_i^2, \tag{10}$$

$$f_{rR}=V_{ij}a_ia_j, \tag{11}$$

with $V_{ii}=D_e$. The eigenstates of both Hamiltonians may be built as a linear combination of products of Morse eigenfunctions as

$$\Psi_{\nu_1\nu_2}=\Phi_{\nu_1}(r_1)\Phi_{\nu_2}(r_2)\ , \tag{12}$$

where $\Phi_{\nu_i}(r_i)$ is the *Morse eigenfunction* given by

$$\Phi_{\nu_i}(r_i)=N_{\nu_i}x^{\beta_i-\nu_i-1/2}\exp\left(-\frac{x}{2}\right)L_{\nu_i}^{2\beta_i-2\nu_i-1}(x)\ , \tag{13}$$

with

$$N_{\nu_i}=\left\{\frac{[a_i(2\beta_i-2\nu_i-1)\nu_i!]}{\Gamma(2\beta_i-\nu_i)}\right\}^{1/2}\ , \tag{14}$$

$$x=2\beta_i\exp(-a_ir_i)\ , \tag{15}$$

$$\beta_i=\frac{1}{a_i\hbar}\sqrt{2\mu_iD_e}\ , \tag{16}$$

$$E_{\nu_i}=-D_e\left[1-\left(\nu_i+\frac{1}{2}\right)\frac{1}{\beta_i}\right]^2\ , \tag{17}$$

where ν_i represents the vibrational quantum number of the Morse oscillator, with the maximum number equal to $\beta_i-\frac{1}{2}$. $L_{\nu_i}^{2\beta_i-2\nu_i-1}(x)$ represents the Laguerre associate polynomial and N_{ν_i} is a normalization factor containing the

gamma function $\Gamma(2\beta_i-\nu_i)$. The matrix elements needed for both Hamiltonians are analytic functions and they can be constructed from the linear combinations of Morse oscillator matrix elements [36].

III. STATISTICAL ANALYSIS

A. General considerations

With the two LM Hamiltonians described above, i.e., the SM and GM models, the vibrational energy levels of the HCN molecule were calculated. This consisted of standard diagonalization of the relevant Hamiltonian, after which the statistical analysis was done. For both models, the statistical analysis has been performed up to 90 000 cm^{-1}. Since the C—H bond dissociation energy is near 42 000 cm^{-1}, the results of the analysis are significant for experimental purposes up to that value. The analysis of the energies above the dissociation limit is of somewhat theoretical interest, even though they may be relevant for studying resonant (predissociating) states in the continuum. This choice allows us to get a clearer comparison between the predictions made between the SM and the GM models. The statistical theory of energy levels is based on *random matrices*, introduced by Wigner to study the complex behavior observed in nuclear spectra [37]. The construction of such matrices, made of independent matrix elements, requires the invariance of the ensemble under orthogonal transformations. This defines the so-called *Gaussian orthogonal ensemble* (GOE). Due to interaction between levels, nuclear [5,38], atomic [39], and molecular [3] spectra show some features of the GOE-type systems, such as *regularity* (i.e., level clustering) and *irregularity* (i.e., level repulsion). Since many reviews about the statistical analysis of energy levels are available [5,10,40–42], we give only a brief description of the statistical measures used in this work. We have utilized two widely used statistical tests: nearest-neighbor level-spacing distribution (NNLSD) and Δ_3 statistics of Dyson and Mehta. Their application to the HCN vibrational spectra permits its characterization by assignment of so-called *correlation properties* [40]. NNLSD represents the most significant test relative to the correlation between nearest levels. We refer to the literature for various derivations [41]. For our purpose, we employed the Brody distribution function [43]

$$P(S)=A\left(\frac{S}{D}\right)^{\omega}\exp\left\{-\left[\frac{S}{D}\,\Gamma\left(\frac{\omega+2}{\omega+1}\right)\right]^{\omega+1}\right\}, \tag{18}$$

where S is the spacing between nearest levels, A a normalizing factor, and D the average spacing of the ensemble. The Brody parameter ω is a function of the strength of the level interaction and it assumes values between 0, corresponding to a Poisson distribution for noninteracting levels, and 1, corresponding to a Wigner distribution for a set of levels characterized by a linear repulsion. The other statistical test utilized, the Δ_3 statistics of Dyson and Mehta, gives us an account of the so-called *spectral rigidity* or, in other words, the long-range correlation of the spectra. The expression that defines Δ_3 [44] is

TABLE I. Parameters for the simple Morse potential for different HCN isotopic species [25].

Parameter	HCN	DCN	$H^{13}CN$	$HC^{15}N$
D_{CH} (eV)	6.384	5.954	6.357	6.344
a_{CH} ($Å^{-1}$)	1.727	1.783	1.732	1.730
D_{CN} (eV)	10.384	11.256	10.639	7.872
a_{CN} ($Å^{-1}$)	2.363	2.259	2.334	2.753
V_{12} (eV)	−0.450	−0.325	−0.486	−0.470

$$\Delta_3(L,j)=\frac{1}{E_{L+j}-E_j}\min_{A,B}\int_{E_j}^{E_{L+j}}[N(E)-AE-B]^2dE\ , \tag{19}$$

$N(E)$ is the staircase function for the levels at energy E; $E_{L+j}-E_j$ represents the energy range containing $L+j$ levels on which the test is performed. For different values of L we have

$$\Delta_3(L)=\overline{\Delta_3(L,j)}\ . \tag{20}$$

The calculated points generally fluctuates between the $L/15$ straight line (no correlation) and the GOE logarithmic curve

$$\Delta_3^{\mathrm{GOE}}(L)=\frac{1}{\pi^2}[\ln L-0.0687]\ . \tag{21}$$

The goodness of the above statistical tests may depend on the *unfolding* or *deconvolution* procedure [10,42]. It consists of the elimination of the so-called "secular behavior" of the spectra, due to the natural variation of the level density with the energy. Among the various methods used for this purpose, we have chosen the polynomial method, that consists of fitting the $N(E)$ function with a polynomial expansion of degree m. The new set of eigenenergies so obtained, characterized by a constant density of levels and an average level spacing, represents the new ensemble to which the above cited statistical tests will be applied.

B. Model I

Let us consider the SM model [25], i.e., Eqs. (6) and (7), whose parameters are listed in Table I. These parameters allowed us to calculate the energy levels of the various isotopes. The number of Morse (i.e., bound) states per oscillator [see Eq. (17)] chosen are 25 and 40 for C—H and C—N bonds, respectively, for all the isotopic species under study, involving diagonalization of 1000×1000 matrices. The very high-energy parts of the spectra were discarded since they would be inaccurate due to the absence of any discrete-continuum coupling. The useful portion of the spectra is then subjected to the unfolding procedure by polynomial fitting.

Consider the vibrational levels for the $H^{12}C^{14}N$ isotopic species. We calculate both the Brody parameter ω for NNLSD as well as the Δ_3 test of Dyson and Mehta (see Table III and Fig. 1). The number of levels considered were 40, 89, 184, 291, 578, and 839 with corresponding maximum energies ($E_{\max}$) of 20 000, 30 000, 42 000, 50 000, 70 000, and 90 000 cm^{-1}, respectively. Up to 20 000 cm^{-1}, the Brody parameter ω is close to 0 (Poisson distribution), which is not surprising since the density of levels in this region of

TABLE II. Parameters for the generalized Morse potential for HCN [26].

$a_{CH}=1.847\ 393\ Å^{-1}$
$V_{11}=5.697\ 14$ eV
$V_{111}=0.475\ 28$ eV
$V_{1111}=8.426\times10^{-3}$ eV
$a_{CN}=2.306\ 172\ Å^{-1}$
$V_{22}=10.994\ 46$ eV
$V_{222}=0.499\ 332$ eV
$V_{2222}=5.954\times10^{-3}$ eV
$V_{12}=-0.307\ 63$ eV
$V_{112}=-9.425\times10^{-6}$ eV
$V_{122}=3.657\times10^{-4}$ eV

the spectra is low. Above about 30 000 cm^{-1}, a significant deviation from the Poisson distribution can be seen with ω at 0.54. At the higher energies, ω steadily increases, reaching 0.89. Since the Wigner distribution, $\omega=1.0$, we see that with the increasing of the density of levels, the NNLSD has a clear tendency towards the Wigner distribution. In Fig. 1 three of the NNLSD histograms are plotted with smooth curves going through them. The transition towards the Wigner distribution is unequivocal. Alongside the calculated values of Δ_3 are plotted as a function of L Figs. 1(d)–1(f). The straight lines representing the Poisson distribution are extremely far from the obtained values of Δ_3 which for almost all L considered lie on the GOE logarithmic curve.

The three isotopic species DCN, $H^{13}CN$, and $HC^{15}N$ were next considered with appropriate diagonalization of the Hamiltonian, i.e., Eqs. (6) and (7), followed by a similar statistical analysis. The values of the Brody parameter ω, for all energy levels above $E_{max}=42\ 000\ cm^{-1}$, are 0.69 (261 levels), 0.32 (195 levels), and 0.67 (201 levels) for DCN, $H^{13}CN$, and $HC^{15}N$ isotopic species, respectively. Comparing the four different isotopes we note that only when the central atom is increased in mass, i.e., ^{12}C is replaced by ^{13}C, does ω get significantly reduced. Since the central mass m_C is inversely proportional to the kinetic coupling term, increase of the mass of the central atom produces a decrease in the coupling, thereby explaining this tendency towards the Poisson distribution as the coupling is reduced. In Fig. 2 both NNLSD and Δ_3 statistics for DCN, $H^{13}CN$, and $HC^{15}N$ are plotted. The most significant of these is that for the isotopic species $H^{13}CN$, the NNLSD histogram is significantly peaked towards lower values of S/D. The corresponding Δ_3 test for low values of L, where it is more significant, shows deviations from the GOE curve and a small tendency towards the $L/15$ straight line. However, this change of the isotope from ^{12}C to ^{13}C has a significant effect on the results of the statistical analysis and can be clearly seen by comparing Fig. 1(b) with Fig. 2(b).

C. Model II

The description of HCN vibrational dynamics by the GM model [26], i.e., Eqs. (8) and (9), is in principle more accu-

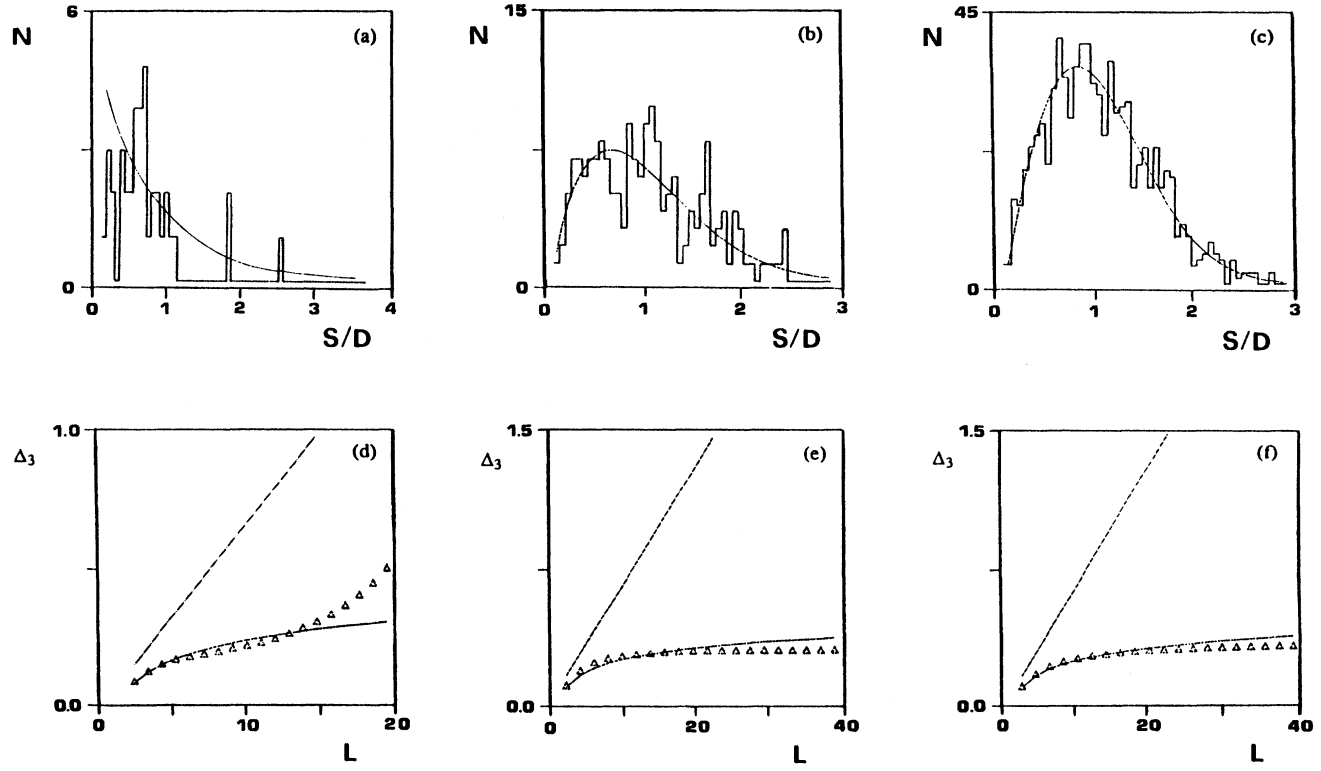

FIG. 1. NNLSD (a)–(c) and Δ_3 statistics (d)–(f) for HCN (SM potential): (a), (d) $E_{max}=20\ 000\ cm^{-1}$; (b), (e) $E_{max}=42\ 000\ cm^{-1}$; (c), (f) $E_{max}=90\ 000\ cm^{-1}$.

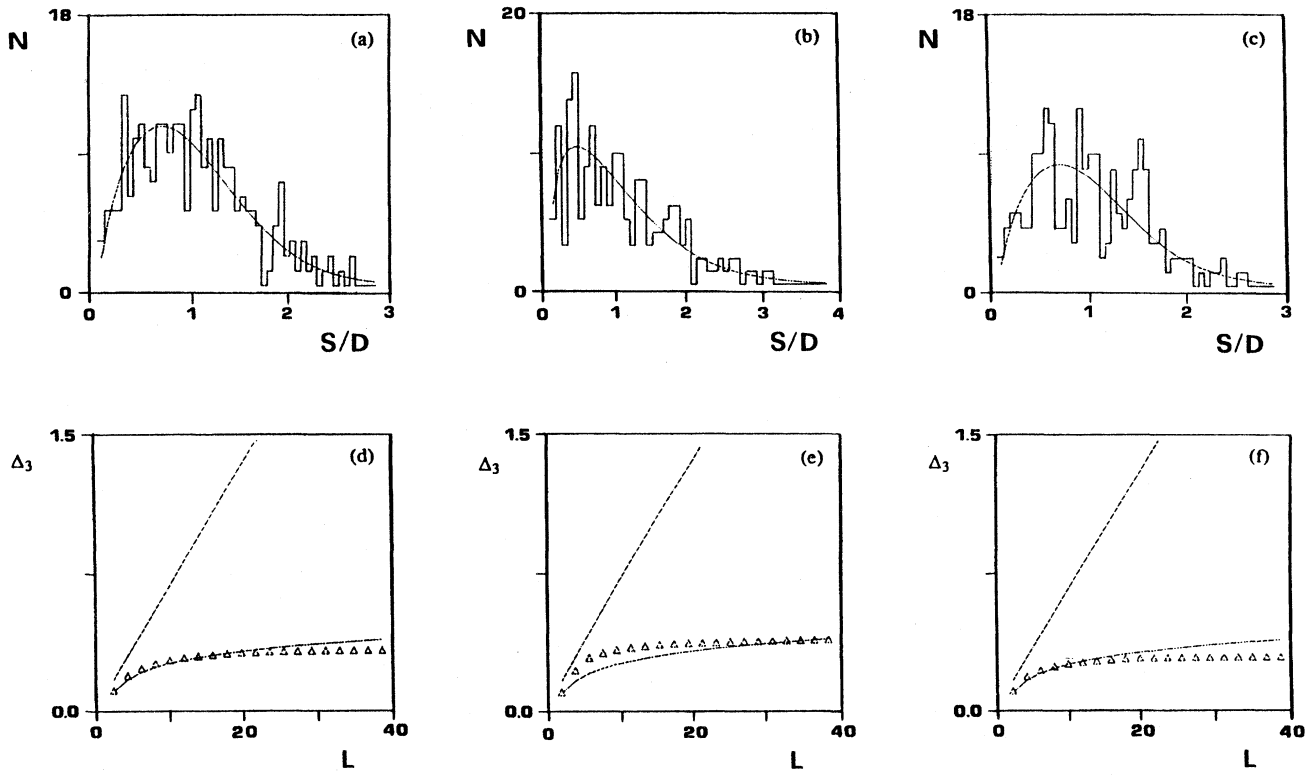

FIG. 2. NNLSD (a)–(c) and Δ_3 statistics (d)–(f) for different isotopic species (SM potential) at $E_{max}=42\,000$ cm^{-1}: (a), (d) DCN; (b), (e) H^{13}CN; (c), (f) HC^{15}N.

rate due to the higher number of experimental levels fitted. The parameters needed are given in Table II. Therefore it is interesting to study the statistical properties of this model and then compare the results with the SM model. The results of the calculation are shown in Table III and Fig. 3. We note first that in the same range of energies, the number of levels are essentially the same, in both SM and GM models. For the GM model, ω starts at 0.12 for the first 40 levels ($E_{max}=20\,000$ cm^{-1}), slowly increasing to 0.14 at $E_{max}=30\,000$ cm^{-1} (88 levels), to 0.22 for $E_{max}=42\,000$ cm^{-1} (186 levels). For $E_{max}=50\,000$ cm^{-1} (283 levels) $\omega=0.35$, for $E_{max}=70\,000$ cm^{-1} (567 levels) $\omega=0.62$, and finally for $E_{max}=90\,000$ cm^{-1} (823 levels) $\omega=0.72$. One does see a slow transition towards the Wigner distribution. It is helpful to utilize the histograms in Figs. 3(a)–3(c) to appreciate how the change of the statistical behavior arises with increasing density of levels. The Δ_3 statistics, which are plotted in Figs. 3(d)–3(f), all show marked deviation from the straight line. The first two curves for low values of L, Δ_3 is linear while for larger L it deviates sharply from the straight line. Since Δ_3 is more significant for small L, one cannot say that for E_{max} up to 42 000 cm^{-1} a Wigner-like behavior has been obtained. For the highest energy ($E_{max}=90\,000$ cm^{-1}) Δ_3 lies completely on the GOE curve through the entire range for L [Fig. 3(f)].

TABLE III. Number of levels (N_{lev}) and Brody parameter (ω) for simple and generalized Morse potentials for HCN, calculated at different values of E_{max}.

	Simple Morse		Generalized Morse	
E_{max} (cm^{-1})	N_{lev}	ω	N_{lev}	ω
20 000	40	0.01	40	0.12
30 000	89	0.54	88	0.14
42 000	184	0.61	186	0.22
50 000	291	0.69	283	0.35
70 000	578	0.83	567	0.62
90 000	839	0.89	823	0.72

It is helpful to get a global picture of variation of the Brody parameter ω with the energy (E_{max}) for the two models (see Fig. 4). Both the models clearly tend toward the Wigner distribution with increasing E_{max}, i.e., with increasing density of levels. The SM model produces a larger value of ω except at very low energies where statistical analysis may not be that significant. One can therefore conclude that both the SM and the GM model produce a similar effect due to interactions between unperturbed levels.

IV. QUANTUM-CLASSICAL CORRESPONDENCE

Since both these two models show an unequivocal tendency towards the Wigner distribution for the energy levels at the higher-energy part of the spectra, it is tempting to correlate such behavior with classical dynamics of the same. In fact, it is possible to characterize the intramolecular dynamics classically utilizing Poincaré sections [45] and Lyapunov exponents [46,47].

Using the Hamiltonian model II [Eqs. (8) and (9)] for the HCN molecule, we have shown previously that the threshold

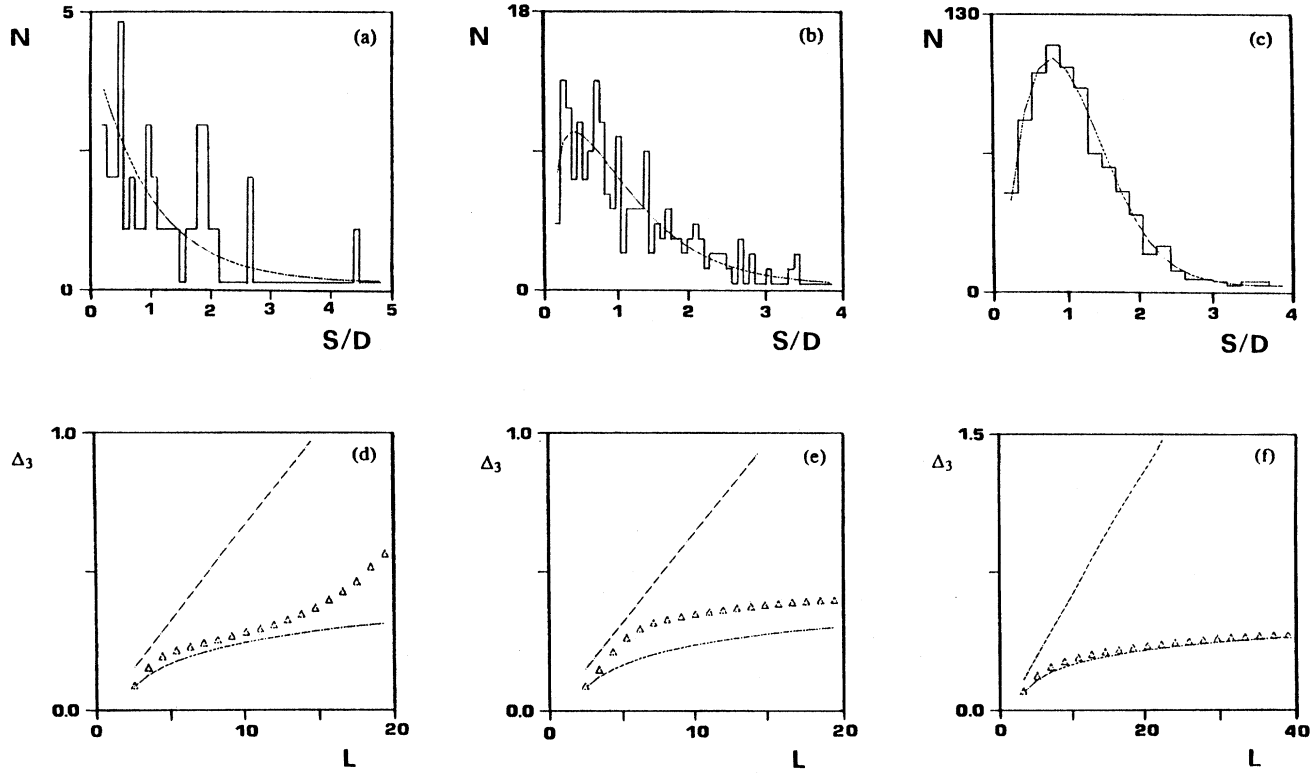

FIG. 3. NNLSD (a)–(c) and Δ_3 statistics (d)–(f) for HCN (GM potential): (a), (d) $E_{max}=20\,000$ cm^{-1}; (b), (e) $E_{max}=42\,000$ cm^{-1}; (c), (f) $E_{max}=90\,000$ cm^{-1}.

energy for chaos lies between 22 585 and 23 391 cm^{-1}. In Fig. 5 we plot the Poincaré sections for three values of energies, calculated for the C—H and C—N bonds, with an identical number of initial conditions. These are Figs. 5(a) and 5(d) at energy of 22 585 cm^{-1}, Figs. 5(b) and 5(e) at 23 391 cm^{-1}, and Figs. 5(c) and 5(f) at 24 198 cm^{-1}. Figures 5(a)–5(c) correspond to the C—H bond calculated at $r_2=0$ and Figs. 5(d)–5(f) refer to the C—N bond calculated at $r_1=0$. At energy of 22 585 cm^{-1}, the Poincaré sections in the two bonds are regular curves and each curve is made up of the intersection of points generated by one initial condition. With the increase of energy, the coupling between moments and positions grows and irregular motion appears [12,13]. At energy of 23 391 cm^{-1}, for certain initial conditions, some erratic points around the regular trajectories tend to appear. At energy of 24 198 cm^{-1}, these random distributions of points are quite dominant. From this analysis it is clear that the irregular motion depends on the initial conditions and the specific value of the control parameter, which determines the molecular energy. At 22 585 cm^{-1}, a large number of trajectories has been calculated and all of these result in regular curves as has been checked by examining the Poincaré sections. For certain initial conditions, the Lyapunov exponent has been calculated and found to be negative (-0.1). For 23 391 cm^{-1}, the irregular curves start to appear and the Lyapunov exponent calculated has been positive with the value 0.3, thereby showing a change of sign between these two energies [12].

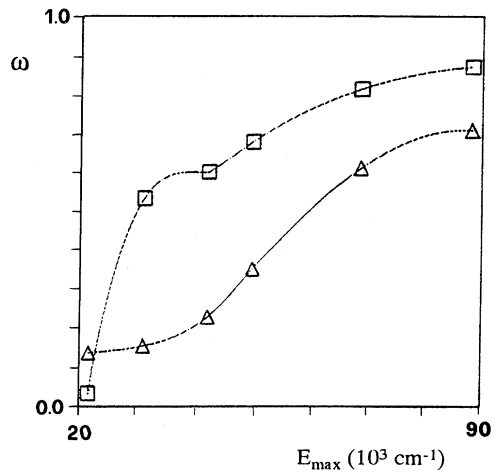

FIG. 4. Brody parameter (ω) vs E_{max} for SM (□) and GM (△) potentials.

Recently we have considered that the isotopic masses of the constituent atoms can be chosen as a control parameter in intramolecular dynamics [12] and have utilized classical dynamics to calculate photodissociation probability for a HCN molecule [48]. In quantum mechanics from a set of eigenvalues, applying random matrix theory, the fluctuations of the spectra are analyzed to determine corresponding statistical ensembles and to assign correlation properties of the eigenvalue spectra. The link between the classical and the quantum analysis is energy. From Table III, one observes that the Brody parameter increases with energy. For low energies,

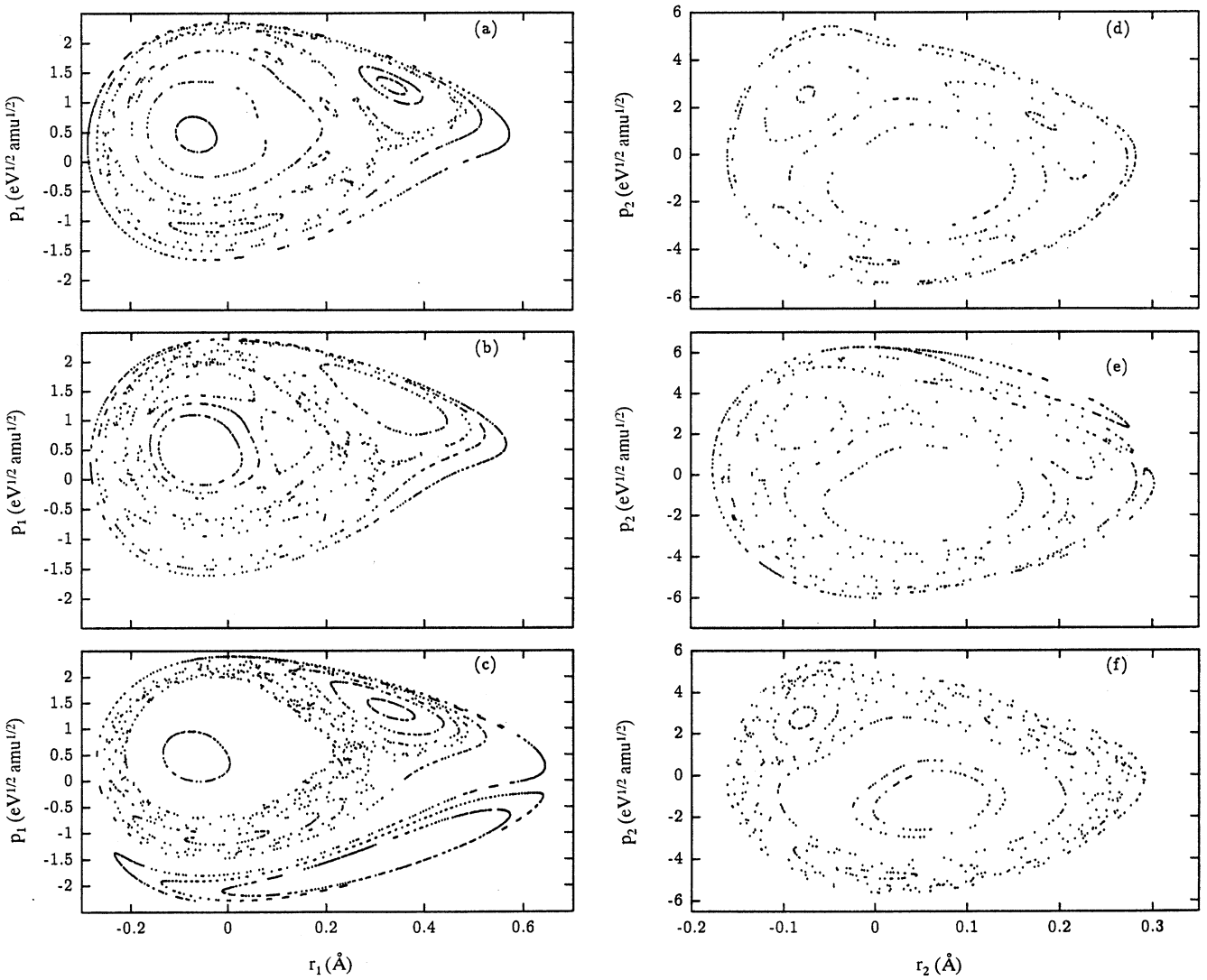

FIG. 5. Poincaré sections at different values of energy: (a), (d) at $E=22\,585$ cm^{-1}, (b), (e) at $E=23\,391$ cm^{-1}, and (c), (f) at $E=24\,198$ cm^{-1}. (a)–(c) for C—H bond at $r_2=0$ and (d)–(f) for C—N bond at $r_1=0$.

necessarily with few eigenvalues, the Brody parameter is close to zero (Poisson distribution) while at higher energies, the Brody parameter tends to that corresponding to the Wigner distribution. The classical mechanical analysis closely follows this qualitative change and the dynamics makes the transition from regular to irregular motion.

V. CONCLUSIONS

In summary, in this work we have utilized two local-mode Hamiltonians to construct theoretical (stretching) vibrational eigenenergies for a HCN molecule at energy domains that have not yet been experimentally explored. We find strong evidence of the role that the kinetic coupling plays in the correlation properties assigned to the corresponding stretching vibrational spectra. Especially clear is the trend towards the Wigner distribution (e.g., the Brody distribution with ω lying far from zero) which signifies how the coupling between the local modes produces strong dynamical effects that are reflected in the statistical properties of the spectra. An effect of the masses of the constituent atoms has also been found. We have made a comparison between the two models which shows that they both produce similar trends, even though with quantitatively different results. Strong correlations have been found between classical chaos and non-Poisson distribution at the higher energies. It should be interesting to test the predictions of these models against experiments.

ACKNOWLEDGMENTS

The authors are grateful to the Centro di Calcolo dell' Università di Trieste for the use of their VAX mainframe computer, to Dr. Alessandro Ferretti (ICQEM-CNR, Pisa) for providing the programs of an earlier study, and to Professor David Farrelly (Utah State University) for a careful reading of the manuscript. J.B. wishes to thank ICTP for financial support.

[1] R. B. Wilson, Jr., J. C. Decius, and P. C. Cross, *Molecular Vibrations, The Theory of Infrared and Raman Vibrational Spectra* (McGraw-Hill, New York, 1955).
[2] S. Califano, *Vibrational States* (Wiley, New York, 1976).
[3] Th. Zimmermann, L. S. Cederbaum, H.-D. Meyer, and H. Koppel, J. Phys. Chem. **91**, 4446 (1987).
[4] M. Quack, Annu. Rev. Phys. Chem. **41**, 839 (1990).
[5] C. E. Porter, *Statistical Theories of Spectra: Fluctuations* (Academic, New York, 1965).
[6] V. Buch, R. B. Gerber, and M. A. Ratner, J. Chem. Phys. **76**, 5397 (1982).
[7] T. Matsushita and T. Terasaka, Chem. Phys. Lett. **105**, 511 (1984); T. Terasaka and T. Matsushita, Phys. Rev. A **32**, 538 (1985).
[8] R. Cimiraglia, A. Ferretti, and N. Rahman, Chem. Phys. Lett. **151**, 38 (1988).
[9] I. Hamilton, J. Chem. Phys. **93**, 8081 (1990).
[10] W. Karrlein, J. Chem. Phys. **94**, 3293 (1991).
[11] F. Pichierri, tesi di Laurea, University of Trieste, 1992.
[12] J. Botina, F. Pichierri, and N. Rahman, Chem. Phys. Lett. **208**, 153 (1993).
[13] J. Botina, F. Pichierri, and N. Rahman, in *Mesoscopic Systems and Chaos*, Proceedings of the Adriatico Research Conference, edited by H. Cerdeira and G. Casati (World Scientific, Singapore, 1994).
[14] F. Pichierri, J. Botina, and N. Rahman, Chem. Phys. Lett. **236**, 543 (1995).
[15] F. Pichierri and N. Rahman, Chem. Phys. Lett. **223**, 275 (1994).
[16] B. R. Henry, Acc. Chem. Res. **10**, 207 (1977).
[17] C. Jaffé and P. Brumer, J. Chem. Phys. **73**, 5646 (1980).
[18] I. A. Watson, B. R. Henry, and I. G. Ross, Spectrochim. Acta **37A**, 857 (1981).
[19] M. S. Child and L. Halonen, Adv. Chem. Phys. **57**, 1 (1984).
[20] A. P. Baronavski, Chem. Phys. Lett. **61**, 532 (1979).
[21] K. K. Lehmann, G. J. Scherer, and W. Klemperer, J. Chem. Phys. **77**, 2853 (1982); **78**, 608 (1983); A. M. Smith, U. G. Jorgensen, and K. K. Lehmann, *ibid.* **87**, 5649 (1987); S. L. Coy, W. Klemperer, A. M. Smith, and K. K. Lehmann, J. Mol. Spectrosc. **134**, 134 (1989).
[22] X. Yang, C. A. Ragashi, and A. M. Wodtke, J. Chem. Phys. **92**, 2111 (1990); J. Opt. Soc. Am. B **7**, 1835 (1990).
[23] P. Botschwina, J. Chem. Soc. Faraday Trans. 2 **84**, 1263 (1988).
[24] J. M. Murrell, S. Carter, and L. Halonen, J. Mol. Spectrosc. **93**, 307 (1982).
[25] J. E. Baggott, G. L. Caldow, and I. M. Mills, J. Chem. Soc. Faraday Trans. 2 **84**, 1407 (1988).
[26] A. M. Smith, W. Klemperer, and K. K. Lehmann, J. Chem. Phys. **94**, 5040 (1991).
[27] B. Gazdy and J. M. Bowman, J. Chem. Phys. **95**, 6309 (1991).
[28] S. Carter, I. M. Mills, and N. C. Handy, J. Chem. Phys. **99**, 4379 (1993).
[29] M. Fournagiotakis, S. C. Farantos, and J. Tennison, J. Chem. Phys. **88**, 1598 (1988); S. C. Farantos and M. Fournagiotakis, Chem. Phys. **142**, 345 (1990).
[30] S. C. Farantos, J. M. Gomez Llorente, O. Hahn, and H. S. Taylor, Chem. Phys. Lett. **166**, 71 (1990).
[31] S. C. Farantos, J. M. Gomez Llorente, O. Hahn, and H. S. Taylor, J. Chem. Phys. **93**, 76 (1990); J. M. Gomez Llorente, S. C. Farantos, O. Hahn, and H. S. Taylor, J. Opt. Soc. Am. B **7**, 1851 (1990); S. C. Farantos, J. M. Gomez Llorente, O. Hahn, and H. S. Taylor, J. Chem. Phys. **94**, 2376 (1991).
[32] Z. Bacic and J. C. Light, J. Chem. Phys. **86**, 3065 (1987); J. C. Light and Z. Bacic, *ibid.* **87**, 4008 (1987).
[33] J. A. Bentley, J.-P. Brunet, R. E. Wyatt, R. A. Friesner, and C. Leforestier, Chem. Phys. Lett. **161**, 393 (1989).
[34] P. M. Morse, Phys. Rev. **34**, 57 (1929).
[35] I. M. Mills and A. G. Robiette, Mol. Phys. **56**, 743 (1985).
[36] F. V. Bunkin and I. I. Tugov, Phys. Rev. A **8**, 601 (1973); J. A. C. Gallas, Phys. Rev. A **21**, 1829 (1980); J. N. Huffaker and L. B. Tran, J. Chem. Phys. **76**, 3838 (1982); V. S. Vasan and R. J. Cross, *ibid.* **78**, 3869 (1983).
[37] E. P. Wigner, SIAM Rev. **9**, 1 (1967).
[38] R. U. Haq, A. Pandey, and O. Bohigas, Phys. Rev. Lett. **48**, 1086 (1982); O. Bohigas, R. U. Haq, and A. Pandey, *ibid.* **54**, 1645 (1983).
[39] N. Rosenzweig and C. E. Porter, Phys. Rev. **120**, 1698 (1960); H. S. Camarda and P. D. Georgopulos, Phys. Rev. Lett. **50**, 492 (1983).
[40] R. Jost and M. Lombardi, in *Quantum Chaos and Statistical Nuclear Physics*, edited by T. H. Seligman and H. Nishioka, Lecture Notes in Physics Vol. 263 (Springer-Verlag, Berlin, 1986), p. 72.
[41] T. A. Brody, J. Flores, J. B. French, P. A. Mello, A. Pandey, and S. S. M. Wong, Rev. Mod. Phys. **53**, 385 (1981).
[42] E. Haller, H. Koppel, and L. S. Cederbaum, Chem. Phys. Lett. **101**, 215 (1983).
[43] T. A. Brody, Lett. Nuovo Cimento **7**, 482 (1973).
[44] F. J. Dyson and M. L. Mehta, J. Math. Phys. **4**, 701 (1963).
[45] D. Farrelly and J. E. Howard, Phys. Rev. A **48**, 851 (1993).
[46] S. C. Farantos, J. M. Gomez Llorente, O. Hahn, and H. S. Taylor, Int. J. Quantum Chem. **24**, 429 (1990).
[47] J. M. Gomez Llorente and E. Pollak, Annu. Rev. Phys. Chem. **43**, 91 (1992).
[48] J. Botina and N. Rahman, Phys. Rev. A **51**, 3088 (1995).